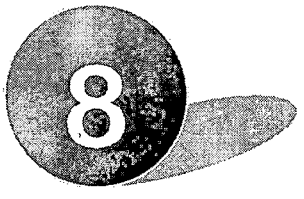

Dasatinib and MSU-H MSNs

Materials and Methods

Mesoporous material MSU-H was procured from Sigma-Aldrich, USA and used for drug loading procedure without further purification.

8.1 Characterization of Mesoporous material MSU-H

MSU-H material was characterized by different instrumental techniques as described in section 6.1.

8.2 Drug-Dasatinib loading in MSU-H MSNs

The drug loading was done with MSU-H MSNs, following the procedure described in section 7.3

8.2.1 Optimization of drug loading procedure

The process of drug loading was optimized with respect to solvent, drug: carrier ratio, temperature, time, and stirring rate.

□*Solvent*

Solvent optimization involves the use of different solvents for drug loading and was checked for % of drug load. The main selection criterion was that the solvent should give optimum solubility of drug and minimum or no solubilization of carrier.

□*Ratio of drug and drug carrier*

Another important parameter is to select proper ratio of drug (DTB) and drug carrier (MSU-H) for maximum entrapment. Different ratio were tried and checked for drug loading.

□*Temperature and time*

Temperature and soaking/stirring time are two important parameters which may affect drug loading. Drug loading procedure was carried out at two different temperature i.e. room temperature and 40° C. Similarly, five different time durations were selected i.e. 6h, 12h, 24h, 48h, and 72h, for drug loading process.

□*Stirring rate*

Rate of stirring also greatly affect the drug loading, hence it is important to optimize the stirring rate. Effect of stirring at higher and normal rate is studied by using magnetic stirrer.

8.2.2 Factorial design for drug loading optimization

3^3 factorial design was used to determine the effect of the three independent factors: the concentration of drug solution, the stirring rate, and drug: carrier weight ratio on the % drug loading of MSU-H MSNs. Each factor was tested at three levels of low, medium and high, designed as -1, 0, and +1 respectively.

Microsoft Excel was used for multiple regression calculation in order to deduce the factors having significant effect on the formulation properties. Three-dimensional response surface plots and two dimensional contour plots resulting from equations were obtained by the NCSS software.

8.2.3 Evaluation of drug loaded MSU-H MSNs

Drug loaded MSNs were evaluated by similar instrumental techniques as described in section 6.1.

8.3 *In-Vitro* dissolution study

In-vitro drug release from the MSNs was studied by the rotating paddle method at 50 rpm (Veego dissolution test apparatus- basket type USP), 37±0.5 °C and in sink conditions. Tests were performed in the following dissolution media[3]: simulated gastric fluid at pH 1.2±0.1, phosphate buffer at pH 4.5±0.1, phosphate buffer at pH 6.8±0.1, simulated intestinal fluid at pH 7.4±0.1 and acetate buffer pH 4 + Triton X-100 (1%) as reported dissolution media[2]. Drug release was monitored for 1h and compared to DTB crystalline powder, the physical mixture and market formulation. Five milliliters of dissolution fluid was removed from the vessel at predetermined intervals and replaced by the same volume of fresh dissolution medium. The samples were filtered through PTFE 0.45 μm filters and DTB content was determined by UV spectrophotometry (λ max = 329 nm for pH 1.2, λ max = 325 nm for pH 4.5, λ max = 325 nm for pH 6.8, λ max = 325 nm for pH 7.4, λ max = 322 nm for reported dissolution media). All experiments were performed in triplicate and the error was expressed as standard deviation.

Results and Discussion

MSU-H MSNs were procured commercially and the material was characterized by different instrumental techniques. The characterization results revealed that the MSU-H MSNs were of prescribed standard. The characterization of mesoporous MSU-H MSNs were discussed in section 6.4. The characterized MSU-H MSNs were used for the drug (dasatinib) loading.

8.4 Drug-Dasatinib loading in MSU-H MSNs

Due to the high specific areas and pore volumes of MSNs, large quantities of drug can be incorporated into the porous MSNs by adsorption to the pore or/and surface of MSNs. The MSU-H MSNs were placed into a concentrated solution of the DTB and stirred magnetically for maximum diffusion of the drug molecules into the mesopores[3] (Fig. 8.1).

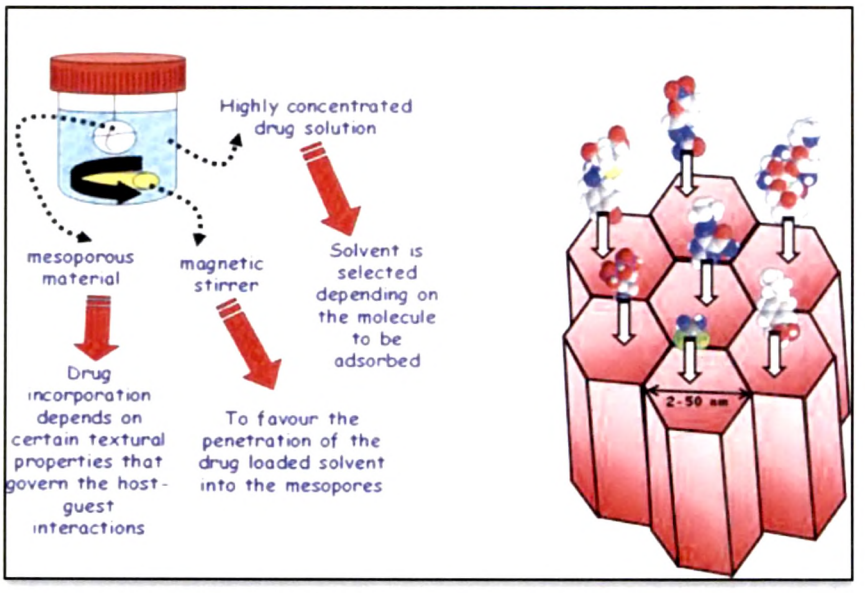

Figure 8.1: Schematic representation of the drug loading procedure

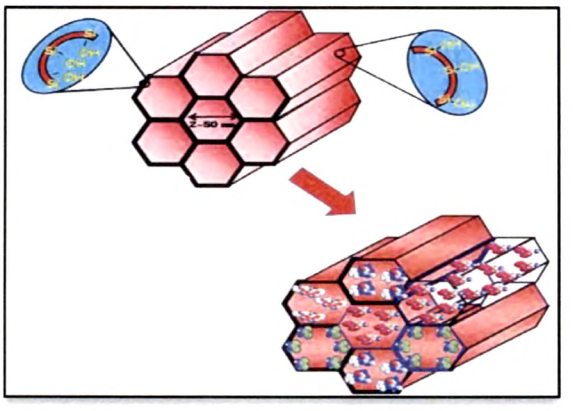

Figure 8.2: Textural properties and drug loading and/or adsorption on MSNs

The MSU-H MSNs have plenty of silanol groups present in to the mesopores and on the surface (Fig. 8.2). The probable mechanism of drug loading is that, the a nitrogen present on piperazine ring of DTB structure would form hydrogen bonds with the silanol groups of MSU-H MSNs and consequently drug molecules would be retained into the mesopores (Fig. 8.3).

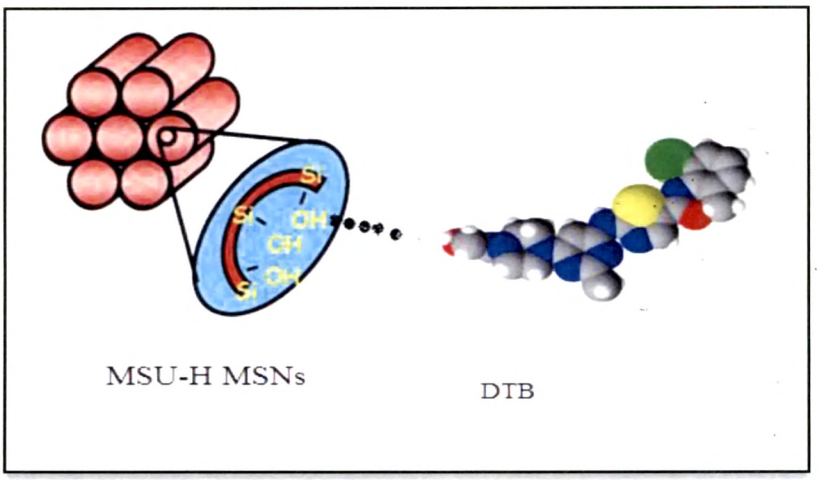

Figure 8.3: DTB linkage to silanol group of MSU-H MSNs

To observe the influence of the different factors, the drug loading process was optimized for solvent, ratio of drug and drug carrier (MSNs), temperature, time and stirring rate, in following section.

8.4.1 Optimization of drug loading procedure

□***Solvent***

For the present study three solvents were tried. As DTB is prominently soluble in acidic media[2], solutions of mineral acids and acidic buffer solutions were tried. Different solvents tried were acetate buffer pH 2.8, 0.1 M HCl and 0.5 M HCl. Drug loading was carried out with these selected solvents and % LE was checked. The results are shown in Table 8.1 and Fig. 8.4.

Table 8.1: Effects of different solvents on MSU-H MSNs drug loading

Solvent used for drug loading	% Drug loading in MSU-H MSNs
Acetate buffer pH 2.8	32. 694
0.1 M HCl	49. 923
0.5 M HCl	48. 878

Results of % LE was suggest that the 0.1 M HCl is appropriate solvent for the drug loading, as it provide maximum loading with comparison to 0.5 M HCl and acetate buffer pH 2.8.

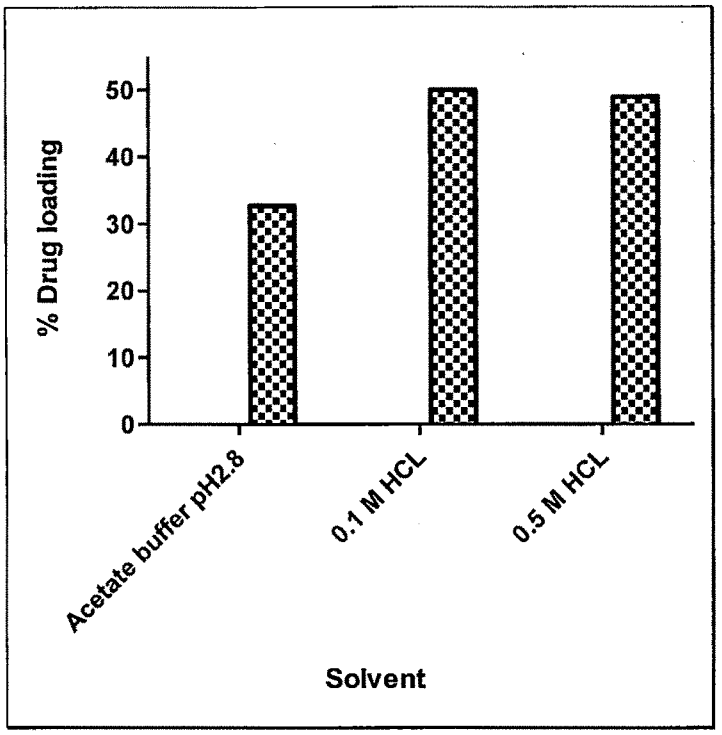

Figure 8.4: Effects of different solvents on MSU-H MSNs drug loading

□***Ratio of drug and drug carrier***

Ratio of drug to MSNs can greatly affects drug loading ability. It was necessary to find out the optimum drug to MSNs ratio. To optimize the ratio, different proportion of MSNs to drug was taken as mentioned in Table 8.2.

Table 8.2: Effects of drug: MSNs ratio on MSU-HMSNs drug loading

Weight Ratio Drug : Carrier	% Drug loading in MSU-H MSNs
1: 0.5	46.085
1:1	49.431
1: 1.5	48.397
1: 2	48.074

Ratio was optimized by taking fixed proportion of drug and variable proportion of MSNs. Four different proportion were selected for MSNs, 0.5, 1, 1.5, and 2. It was found that maximum drug entrapment was achieved with 1: 1 weight ratio. The optimization data graphically present in Fig. 8.5.

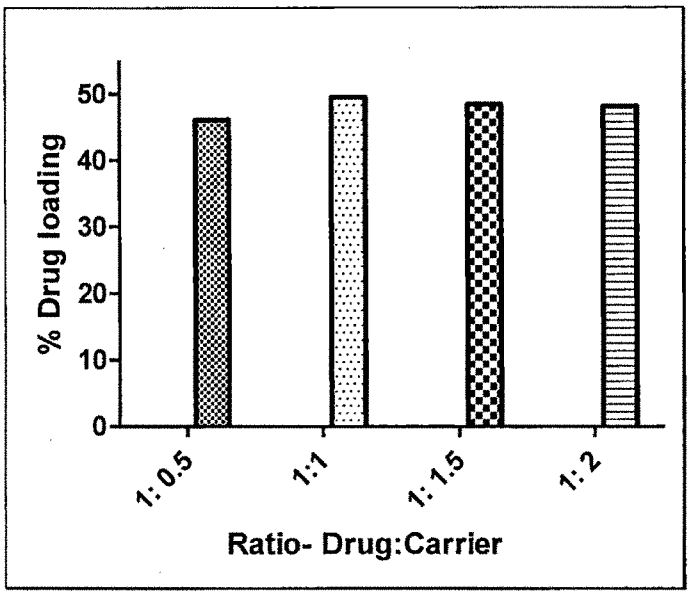

Figure 8.5: Effects of drug: MSNs ratio on MSU-H MSNs drug loading

□*Temperature and time*

The loading process was carried out at two different temperatures i.e. room temperature and 40° C. Similarly five different time durations were selected for proper agitation during the loading process. Stirring was provided with magnetic stirrer for five different time duration, i.e. 6h, 12h, 24h, 48h, and 72h. The results are summarized in Table 8.3 and Fig. 8.6.

Table 8.3: Effects of temperature and time on MSU-H MSNs drug loading

Temperature	% of Drug loading at different time duration				
	6h	12h	24h	48h	72h
Room temp.	43. 543	49. 398	48. 410	48. 270	48. 101
40° C	41. 547	42.765	40. 325	39. 448	39. 254

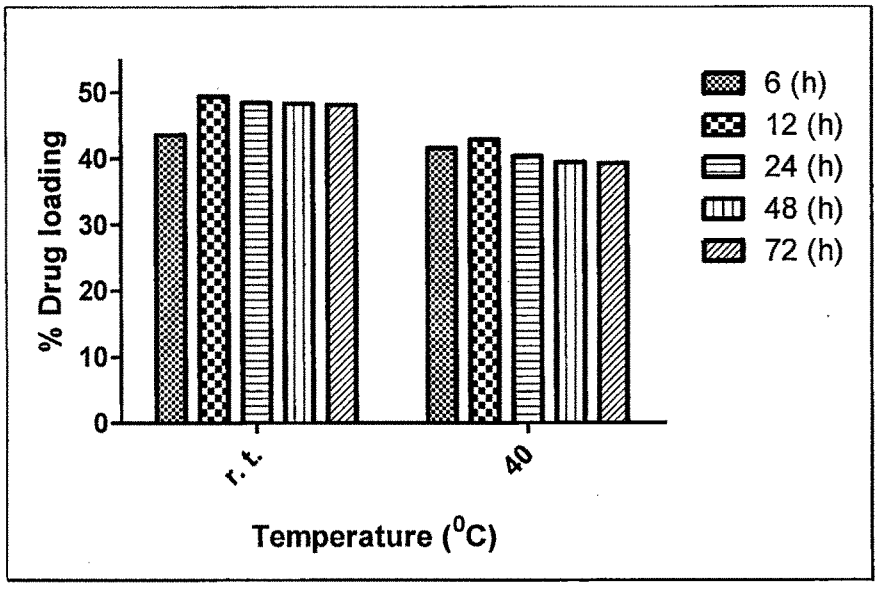

Figure 8.6: Effects of temperature and time on MSU-H MSNs drug loading

The results of % LE revealed that maximum drug loading was attainable if the MSNs and DTB were continuously agitated at least for 12h.

The results of drug loading at 40° C suggested that the elevated temperature was not suitable for the high loading. Higher temperature may increase the DTB solubilization but at elevated temperature the DTB molecules may experience high Brownian motion[6-8] which may not allow the easy diffusion and adsorption in the mesopores of MSU-H MSNs.

□*Stirring rate*

During the loading process, the solution is continuously stirred using magnetic stirrer to improve access of the concentrated solution to the mesopores[7]. MSNs sample was added in drug solution with vigorous stirring and vigorous stirring was continued for 1h, followed by gentle stirring for 11h.

Vigorous stirring was provided at 800 rpm, whereas the gentle stirring rate was optimized at four levels i.e. 50 rpm, 100 rpm, 200 rpm and 400 rpm. The results are summarized in Table 8.4 and Fig. 8.7. The results revealed that as stirring rate was increased from 100 rpm to 400 rpm; the rate of drug loading was deceased from 49 to 45%. Optimized stirring rate data suggested that for the maximum drug loading the stirring should be 100 rpm.

Table 8.4: Effects of stirring rate on MSU-H MSNs drug loading

Stirring speed	~50 rpm	~100 rpm	~200 rpm	~400 rpm
% Drug loading	47.658	49. 620	44. 724	31. 629

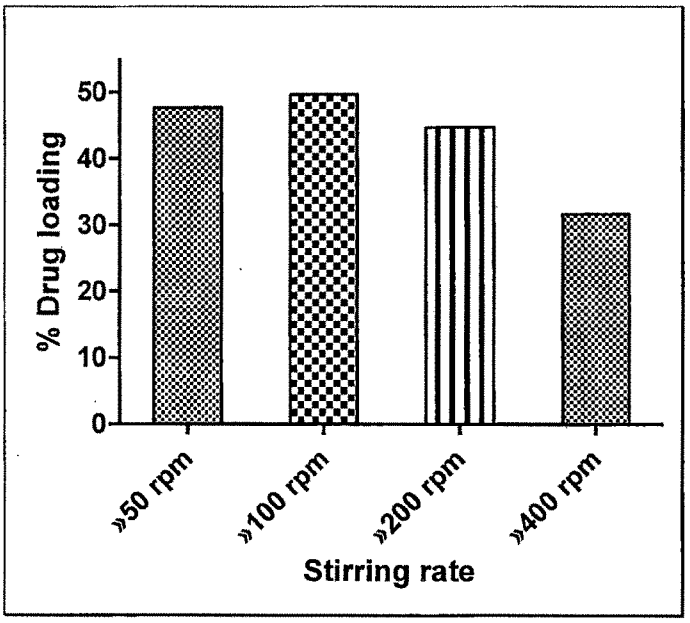

Figure 8.7: Effects of stirring rate on MSU-H MSNs drug loading

8.4.2 Factorial design for drug loading optimization

A statistical model was developed to study the effect of stirring rate, weight ratio of drug: carrier and concentration of drug solution on formulation characteristics.

8.4.2.1 Preparation of batches and optimization by factorial design

Twenty-seven batches of DTB loaded MSU-H MSNs (as a carrier) were prepared using 3^3 factorial design by varying three independent variables the concentration of drug solution (X1), the stirring rate (X2), and drug: carrier ratio (X3). Each factor was tested at three levels of low, medium and high, designed as -1, 0, and +1 respectively. The normalized factor levels of independent variables are given in Table 8.5.

Table 8.5: Factorial 3^3: factors, their levels, and transformed values

Variables with transformed value	Levels		
	Low (-1)	Medium (0)	High (1)
(X1) Concentration of drug solution (mg/ml)	1	5	20
(X2) Stirring rate (rpm)	10	50	100
(X3) Ratio drug: carrier	0.25	0.5	1

The % DTB loading efficiency (response variable) of the prepared batches was determined (Table 8.6) and the highest percent drug loading achieved in mesoporous MSU-HMSNs was 50. 167% at 1 level of X1 (20 mg/ml), 1 level of X2 (100 rpm), and 1 level of X3 (1:1 weight ratio). The results were subjected to multiple-regression analysis. The fitted equation related to percent loading efficiency and transformed factors shows in Eq. (1).

$$Y = 21.201 + 11.036X1 + 6.189X2 + 3.888X3 + 0.163X1^2 + 2.418X2^2 + 1.564X3^2 + 1.771X1X2 + 2.358X1X3 - 0.765X2X3 - 1.622X1X2X3 \quad (1)$$

The data clearly indicated that percent loading efficiency is more dependent on the concentration of drug solution and the stirring rate than the ratio of drug: carrier. The value of correlation coefficient (r) was found to be 0.978, indicating a good fit. The small values of coefficients of terms $X1^2$, $X3^2$, X1X2, X2X3, and X1X2X3 (Eq. 2), were least contributing in loading of DTB in MSU-H MSNs ($p>0.05$). Hence, they were omitted to evolve the reduced model (Eq. 2). The summary of regression analysis is shown in Table 8.7

$$Y = 23.965 + 11.036X1 + 6.189X2 + 3.888X3 + 2.358X1X3 \quad (2)$$

The positive sign for the coefficient of X1, X2, and X3 in Eq. (2) showed that the percent drug loading can be increased by an increase in X1, X2, and X3. The results of ANOVA of the second-order polynomial equation are given in Table 8.7.

Table 8.6: Different batch with their experimental coded level of variables for 3^3 factorial design

Batch code	X1= Concentration of drug solution	X2= Stirring rate	X3= Ratio drug: carrier	% drug loading
M1	-1	-1	-1	6.654
M2	-1	-1	0	7.741
M3	-1	-1	1	9.657
M4	-1	0	-1	10.059
M5	-1	0	0	12.587
M6	-1	0	1	14.548
M7	-1	1	-1	16.225
M8	-1	1	0	18.557
M9	-1	1	1	20.824
M10	0	-1	-1	18.458
M11	0	-1	0	19.556
M12	0	-1	1	20.867
M13	0	0	-1	20.945
M14	0	0	0	22.115
M15	0	0	1	26.852
M16	0	1	-1	27.229
M17	0	1	0	28.454
M18	0	1	1	30.237
M19	1	-1	-1	20.926
M20	1	-1	0	22.817
M21	1	-1	1	40.567
M22	1	0	-1	25.598
M23	1	0	0	28.923
M24	1	0	1	39.556
M25	1	1	-1	41.654
M26	1	1	0	45.557
M27	1	1	1	50.167

Table 8.7: Analysis of variance (ANOVA) of variables for full and reduced model of MSU-H MSNs

	DF	SS	MS	F	R	R^2	Adj.R^2
Regression							
FM	10	3288.915	328.891	35.403	0.978	0.956	0.929
RM	4	3173.235	793.308	66.029	0.960	0.923	0.909
Error							
FM	16	148.637	9.289				
RM	22	264.317	12.014				

[SSE2–SSE1 = 264.317–148.637= 115.68
No. of parameters omitted = 06
MS of error (full model) = 9.289
F calculated = (SSE2–SSE1/no. of parameters omitted)/MS of error (full model)
= (115.680/6)/9.289 = 2.075
Tabled F value = 2.74 (α = 0.05, V1 = 6, and V2 = 16).
a Where DF indicates degrees of freedom; SS sum of square; MS mean sum of square and F is Fischer's ratio].

F-Statistic of the results of ANOVA of full and reduced model confirmed omission of non-significant terms of Eq. (1) and (2). Since the calculated F value (2.07) was less than the tabled F value (2.74), it was concluded that the neglected terms do not significantly contribute in the prediction.

The goodness of fit of the model was checked by the determination coefficient (R^2). In this case, the values of the determination coefficients (R^2) and adjusted determination coefficients (adj R^2) were very high (>90%), which indicates a significance of the model. All the above considerations indicate an adequacy of the regression model[10, 11].

8.4.2.2 Contour plots

Figure 8.8 (a–i) is the contour plot for MSU-H MSNs which were found to be linear and signifying linear relationship between variables X1, X2, and X3. It was observed from contour plots (Fig. 8.8-c) that maximum LE (50.167%) could be obtained with X2 between 0.7 level (70 rpm) to 1 level (100 rpm) and X3 between 0.5 level (0.5:1) to 1 level (1:1). Fig. 8.8-f revealed that maximum loading could be obtained with X1 between 0.6 level (16 mg) to 1 level (20 mg) and X3 between 0.5 level (0.5:1) to 1 level (1:1). Fig. 8.8-i showed that maximum loading could be obtained with X1 between 0.6 level (16 mg) to 1 level (20 mg) and X2 between 0.5 level (50 rpm) to 1 level (100 rpm).

All the two-dimensional contour plots were found to follow the linear relationship between X1, X2, and X3 variables. From the contour, it was observed that higher drug concentration (20 mg/ml), maximum stirring rate (100 rpm), and unit ratio of drug:carrier are necessary for maximum drug loading.

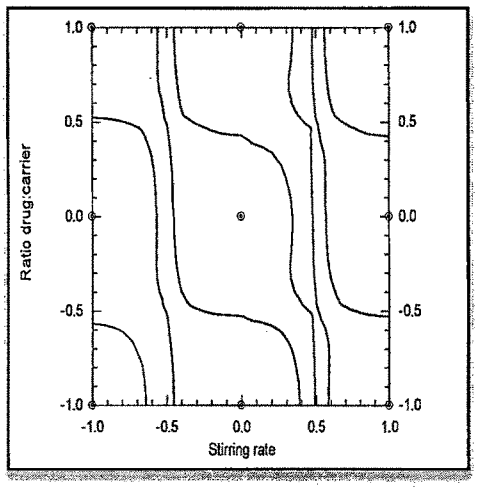

(a) Effect on LE at -1 level of X1

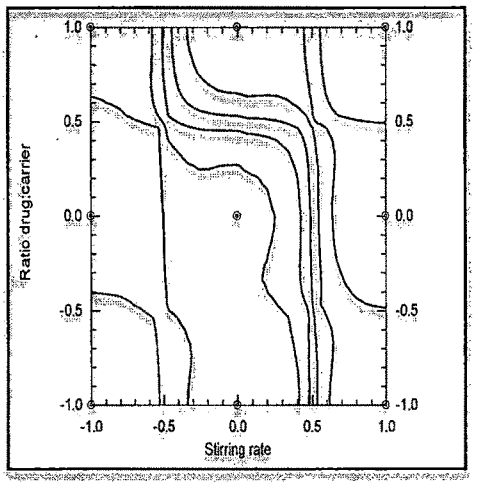

(b) Effect on LE at 0 level of X1

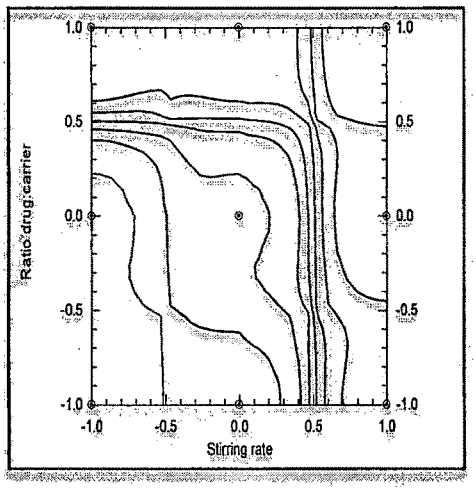

(c) Effect on LE at +1 level of X1

Figure 8.8 (a-c): Contour plots: Effect on LE at -1, 0 and +1 levels of drug concentration (X1)

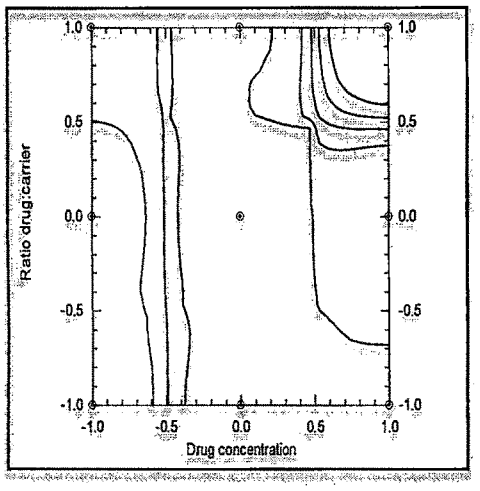

(d) Effect on LE at -1 level of X2

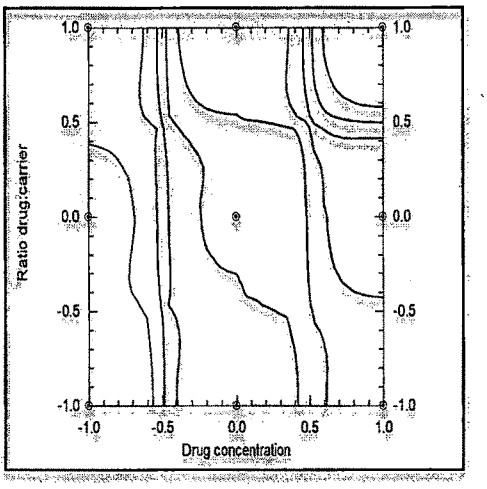

(e) Effect on LE at 0 level of X2

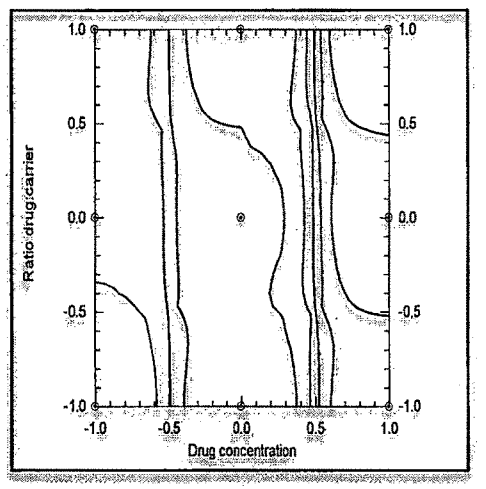

(f) Effect on LE at +1 level of X2

Figure 8.8 (d-f): Contour plots: Effect on LE at -1, 0 and +1 levels of stirring rate (X2)

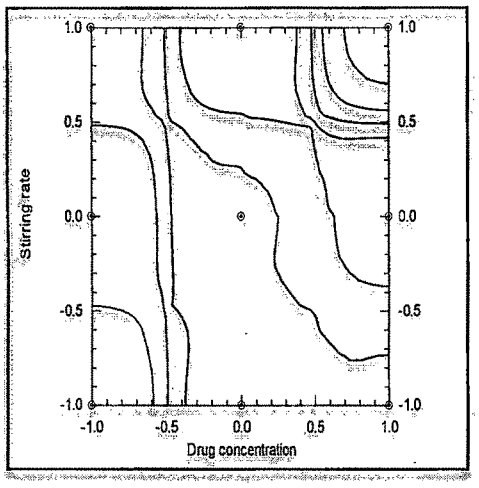

(g) Effect on LE at -1 level of X3

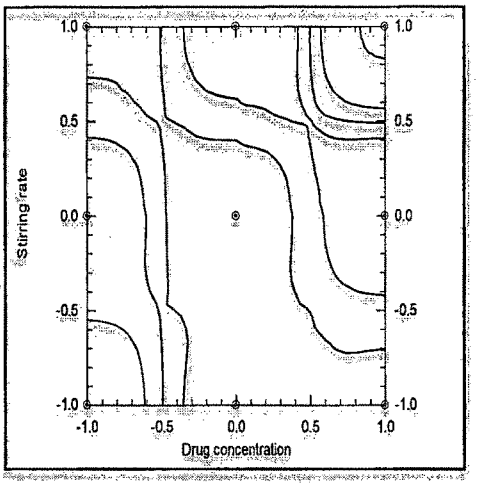

(h) Effect on LE at 0 level of X3

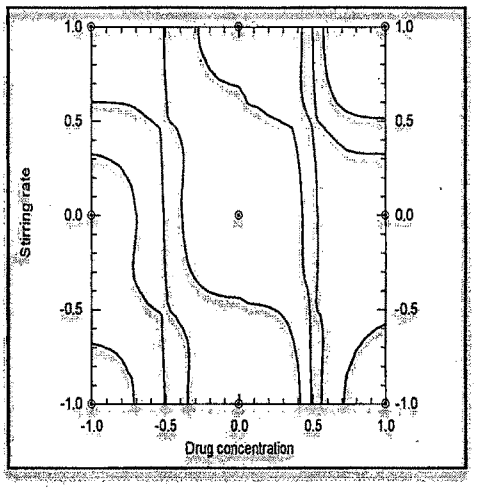

(i) Effect on LE at +1 level of X3

Figure 8.8 (g-i): Contour plots: Effect on LE at -1, 0 and +1 level of drug: carrier ratio (X3)

8.4.2.3 Response surface plots

Three-dimensional response surface plots generated by the NCSS software are presented in Fig. 8.9 (a-i), for MSU-H MSNs. Fig. 8.9 (a-c) depict response surface plots for LE of MSU-H MSNs at constant level of the factor X1 showing an increase in LE with increase in the stirring rate and increase in weight ratio of drug:carrier. Fig. 8.9 (d-f) depict response surface plots for LE at constant level of the factor X2 indicating an increase in LE with increase in the drug concentration and increase in weight ratio of drug: carrier. Fig. 8.9 (g-i) depict response surface plots for LE at constant level of the factor X3 suggesting an increase in drug concentration and increase in stirring rate increases the LE.

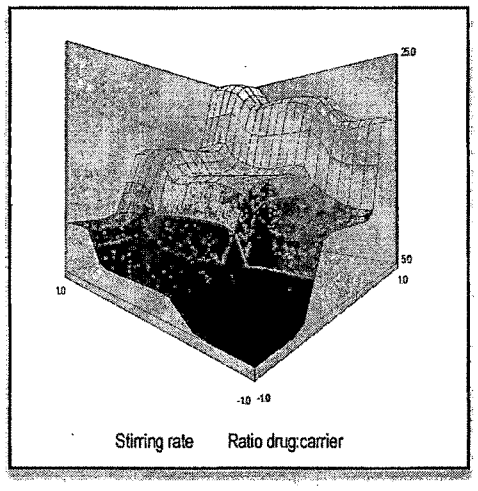

(a) Effect on LE at -1 level of X1

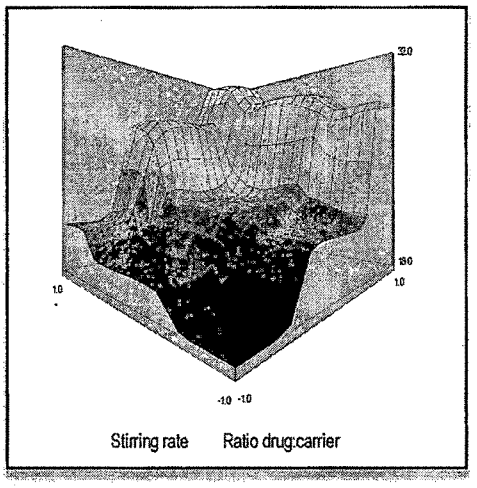

(b) Effect on LE at 0 level of X1

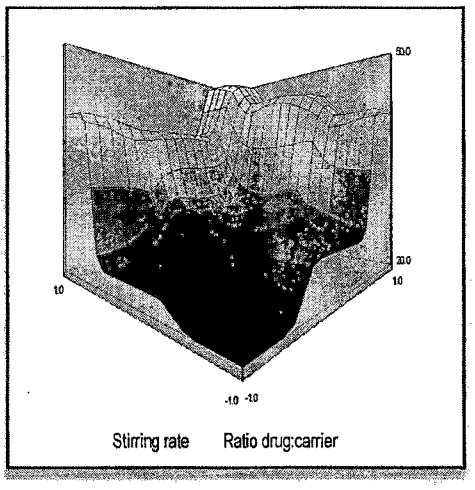

(c) Effect on LE at +1 level of X1

Figure 8.9 (a-c): Response surface plots: Effect on LE at -1, 0 and +1 level of drug concentration (X1)

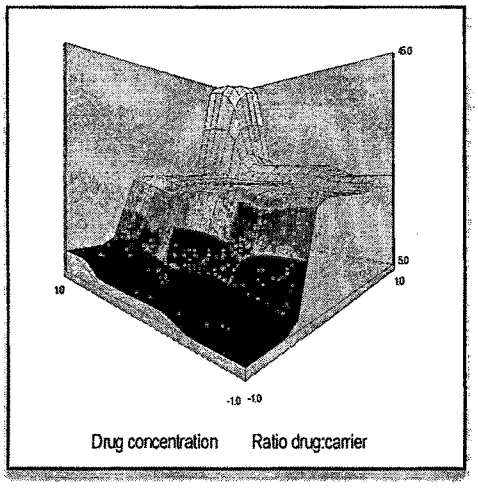

(d) Effect on LE at -1 level of X2

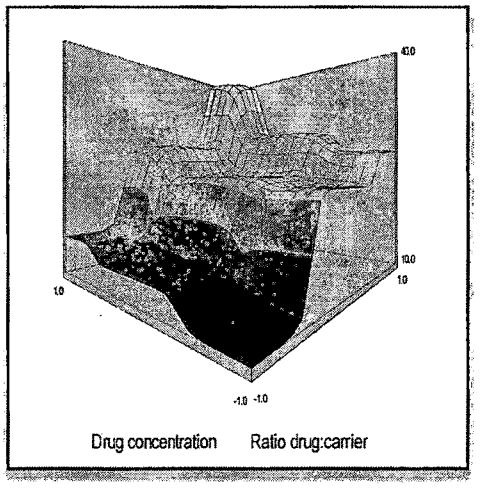

(e) Effect on LE at 0 level of X2

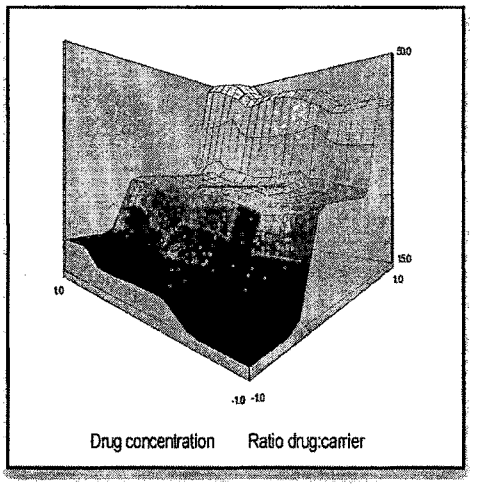

(f) Effect on LE at +1 level of X2

Figure 8.9 (d-f): Response surface plots: Effect on LE at -1, 0 and +1 level of stirring rate (X2)

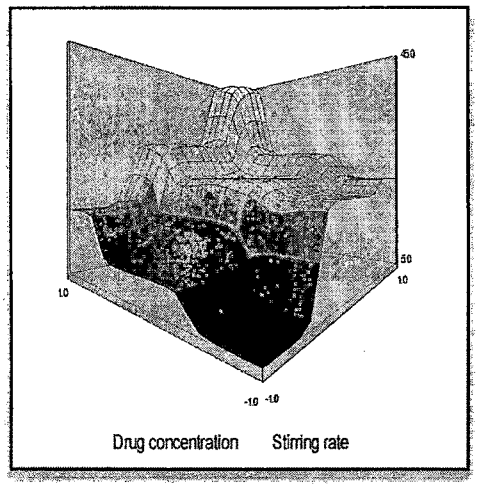

(g) Effect on LE at -1 level of X3

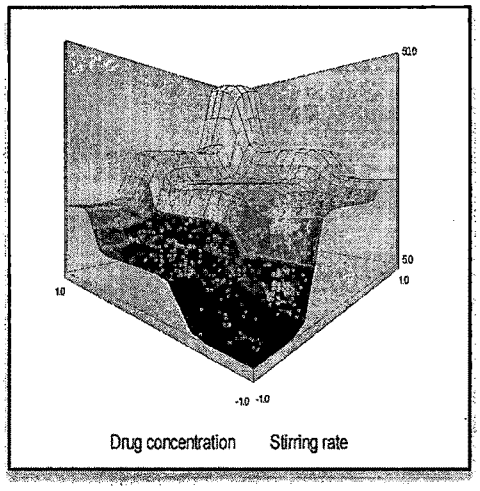

(h) Effect on LE at 0 level of X3

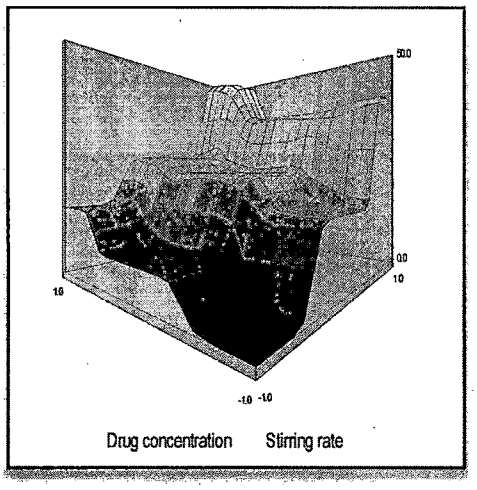

(i) Effect on LE at +1 level of X3

Figure 8.9 (g-i): Response surface plots: Effect on LE at -1, 0 and +1 level of drug: carrier ratio (X3)

8.4.3 Evaluation of drug loaded MSU-H MSNs

Drug loaded MSNs were evaluated for maximum drug loading and intact mesoporosity. Different instrumental techniques like TEM, XRD, nitrogen adsorption, FTIR and DSC were used for this purpose.

8.4.3.1 Transmission electron microscopy (TEM)

The first step was to check that the mesostructure of the MSU-H MSNs has survived after the loading process. The MSNs sample was analyzed by TEM. The high resolution TEM images confirmed the prevalence of the ordered mesostructure after the loading step (Fig. 8.10). TEM Images are marked with some dark spots, which may be the indicative of the confinement of drug molecules within the pores.

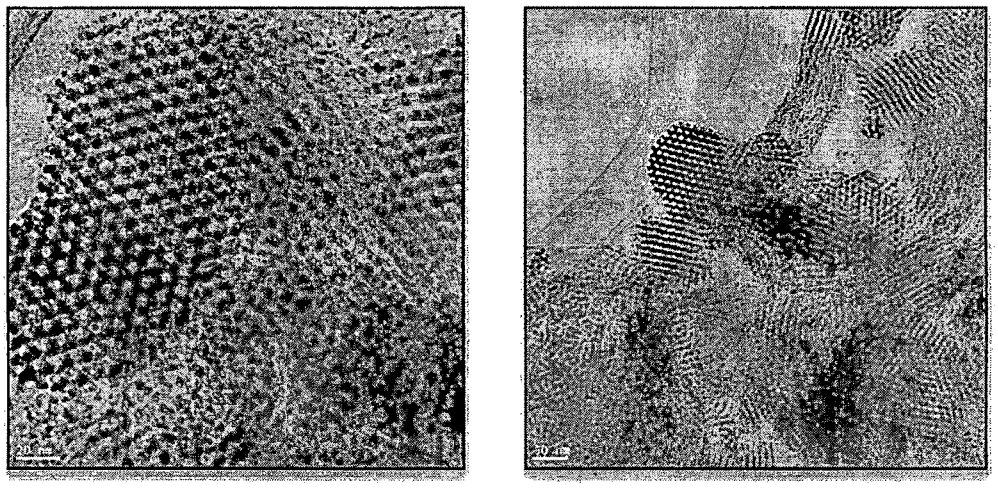

Figure 8.10: TEM images of MSU-H MSNs after drug loading

8.4.3.2 Powder X-ray diffraction (XRD)

The survival of mesoporosity of the MSNs was further confirmed by XRD. For this purpose, a small angle XRD pattern was carried out before and after the loading process (Fig. 8.11 and 8.12).The mesoporous structure of the MSU-H MSNs was confirmed by the diffraction peaks at 100. The same characteristic diffraction peak was observed in MSNs even after the drug loading process. The presence of peaks was indicated that the mesostructure of MSNs was not disturbed after the drug loading. The XRD pattern of DTB is also shown in Fig. 8.12. The drug loaded MSNs show lack of DTB characteristic peaks in XRD pattern further confirming the entrapment of drug molecules within the mesopores.

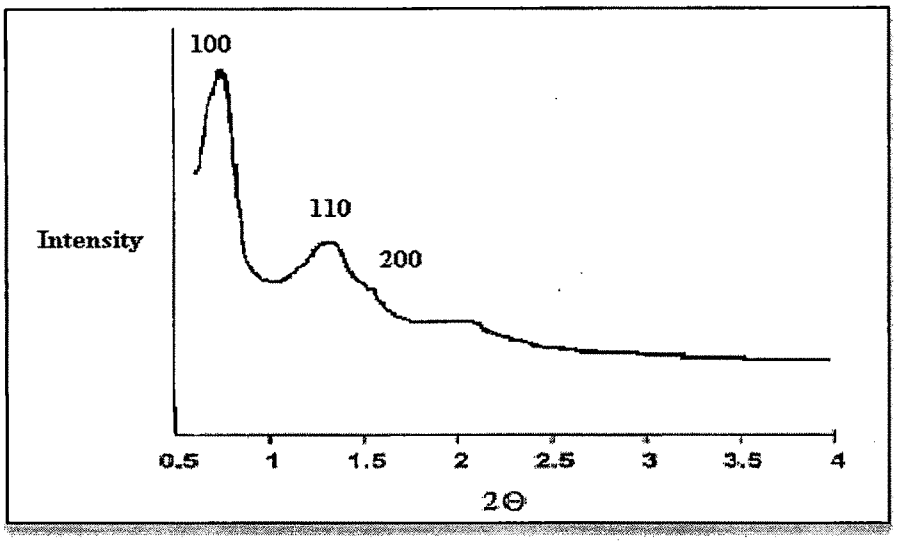

Figure 8.11: XRD pattern of MSU-H MSNs before the drug loading

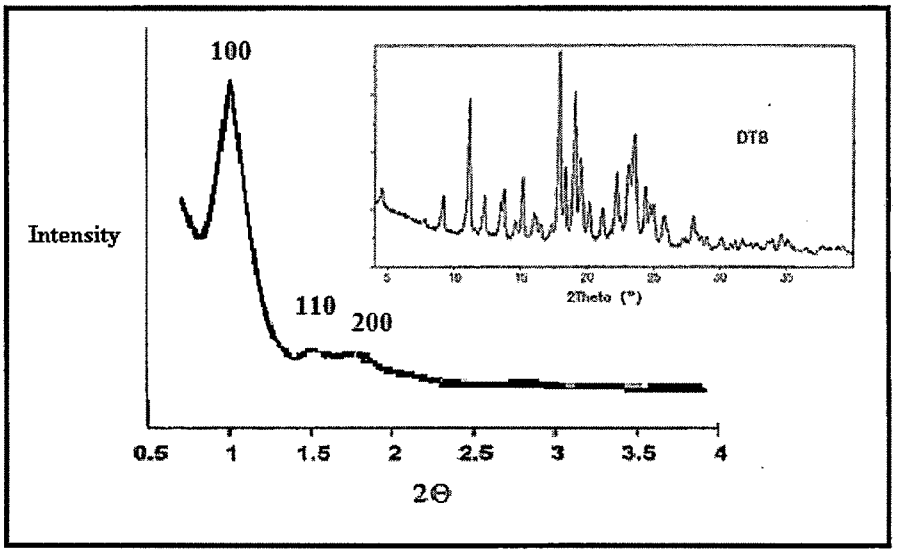

Figure 8.12: XRD pattern of DTB and MSU-H MSNs after the drug loading

8.4.3.3 Nitrogen adsorption isotherm (BET surface analysis)

In Fig. 8.13 and 8.14 nitrogen adsorption-desorption isotherms of MSU-H MSNs before and after the drug loading are reported. Both the isotherm of MSU-H MSNs show typical type IV isotherm according to IUPAC classification representing the mesoporosity. Both the isotherms recorded for MSU-H MSNs also show a hysteresis loop at high relative pressure, which has been ascribed to the presence of interparticle porosity[12].

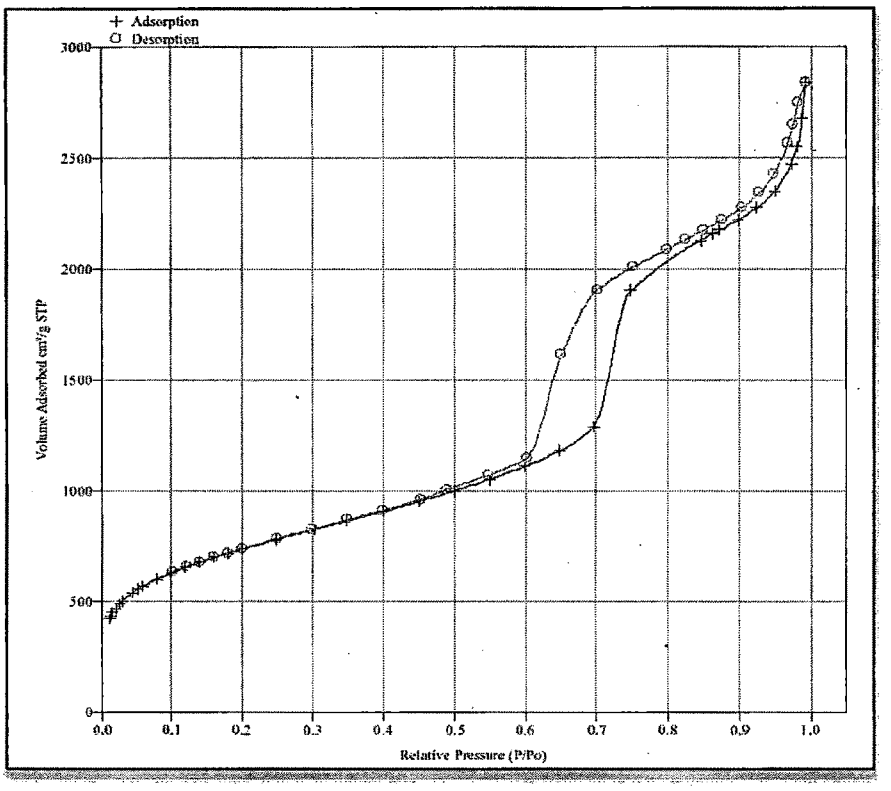

Figure 8.13: Nitrogen adsorption isotherm of MSU-H MSNs before the drug loading

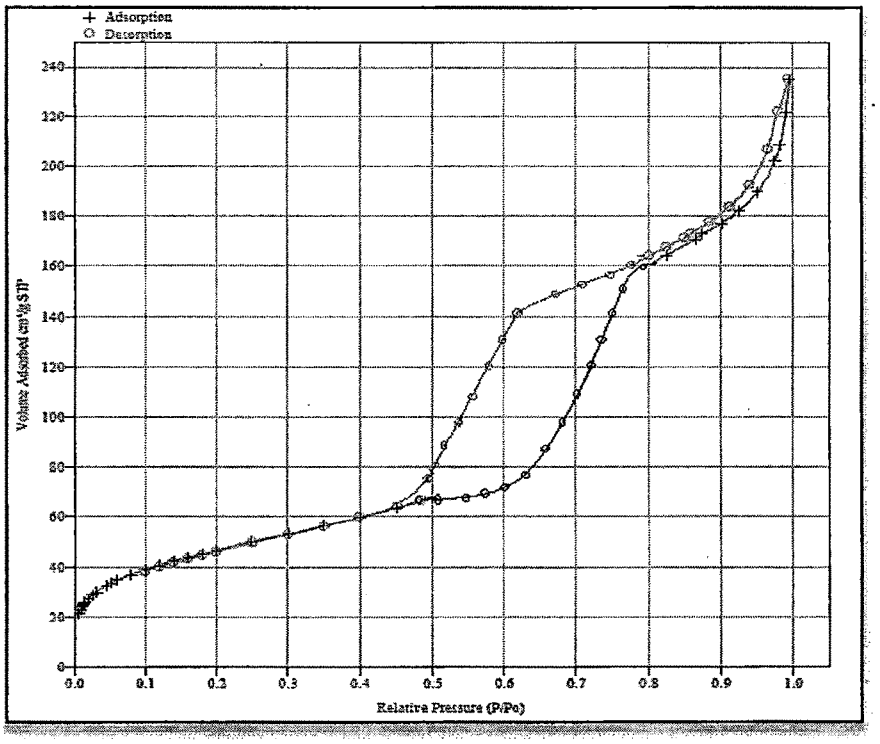

Figure 8.14: Nitrogen adsorption isotherm of MSU-H MSNs after the drug loading

The calculated B.E.T. specific surface area for MSU-H MSNs alone and MSU-H MSNs after DTB loading were found to be 644.02 and 171.06 m^2/g, respectively. The adsorption isotherms of DTB loaded MSNs showed that the adsorbed nitrogen volume decreased after drug loading. Correspondingly, the average pore size distribution for drug loaded MSU-H MSNs, calculated by the BJH–KJS method, was shifted from 7.29 nm to 4.58 nm and the mesopore volume decreased from 0.821 to 0.472 cm^3/g for the primitive MSU-H MSNs and drug loaded MSU-H MSNs, respectively (Fig. 8.15). Numerical data for MSU-H MSNs and drug loaded MSU-H MSNs is shown in Table 8.8.

Table 8.8: Pore diameter, volume and BET surface area of MSU-H MSN

MSNs	Pore diameter (nm)	Pore volume (cm^3/g)	S_{BET} (m^2/g)
MSU-H	7.291	0.821	644.021
DTB loaded MSU-H	4.582	0.472	171.064

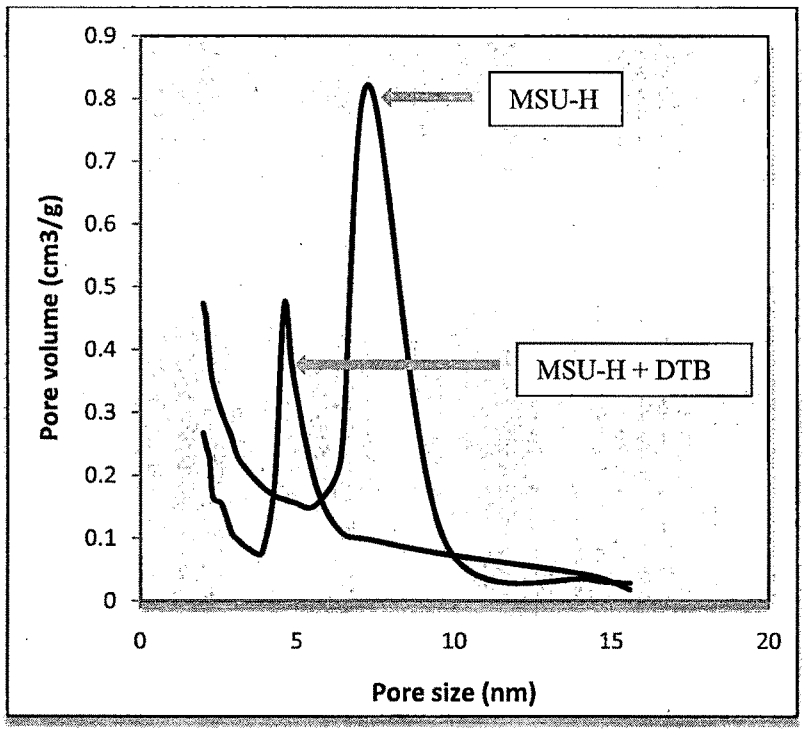

Figure 8.15: Pore size distribution and pore volume of MSU-H MSN before and after drug loading

8.4.3.4 FTIR analysis

FTIR spectrum of MSU-H MSNs (Fig. 8.16) showed the presence of a vibration band at 3747 cm^{-1} attributable to isolated terminal silanol groups and of another large band at 3452 cm^{-1} attributable to geminal and associated terminal silanol groups. The stretching vibrations of Si-O-Si and Si-OH can be seen at 1083 and 968 cm^{-1}. The FTIR spectral analysis of DTB powder (Fig. 8.17) showed the principal peaks at about 772 cm^{-1} (aryl C-Cl stretching), 1184 cm^{-1} (– C=S stretching), 1573 cm^{-1} (-CO-NH), 1621 cm^{-1} (-CO stretching of –CO-NH) 1452, 1505 cm^{-1} (aryl system), 809 cm^{-1} (aromatic ring system), and 2944 cm^{-1} (-OH stretching) confirming the purity of the drug. The spectrum of drug loaded MSU-H MSNs (Fig. 8.18) shows a remarkable absence of the characteristic peaks DTB pure sample, suggesting that majority of DTB was entrapped in MSNs.

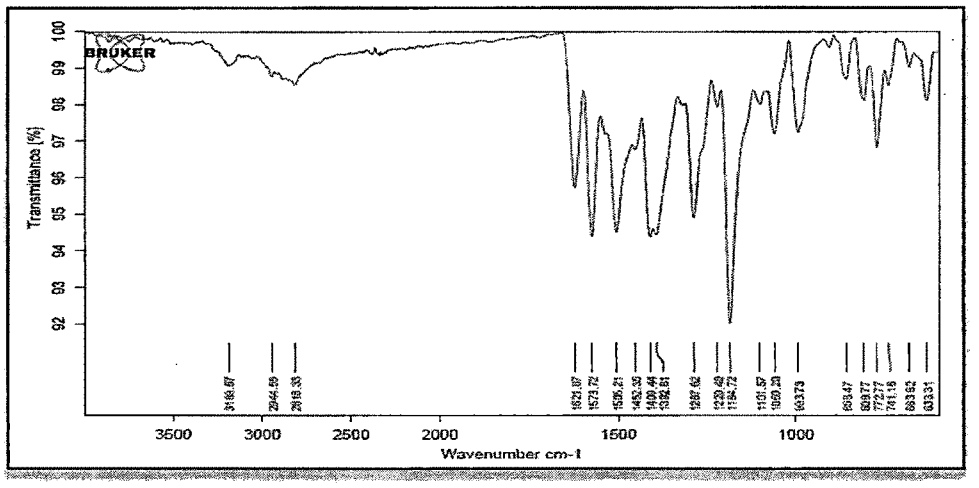

Figure 8.17: FTIR spectra of DTB

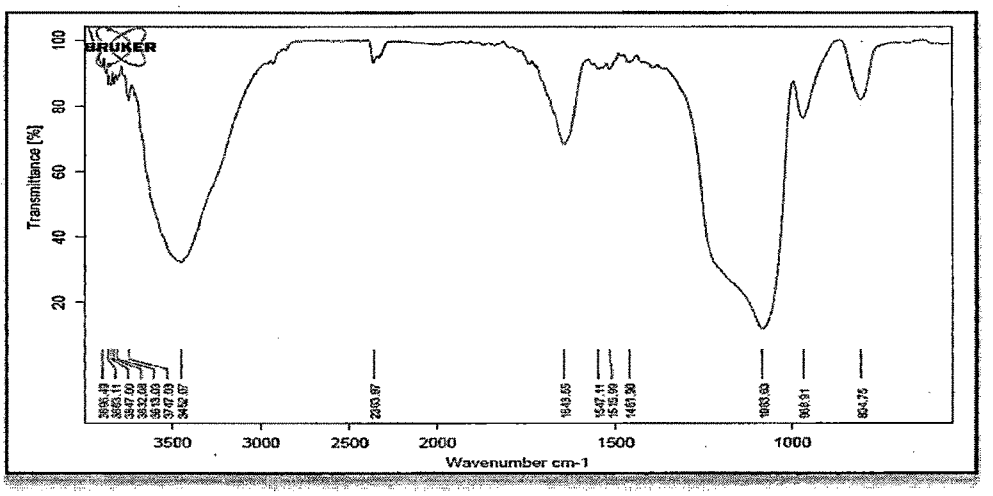

Figure 8.16: FTIR spectra of MSU-H MSNs

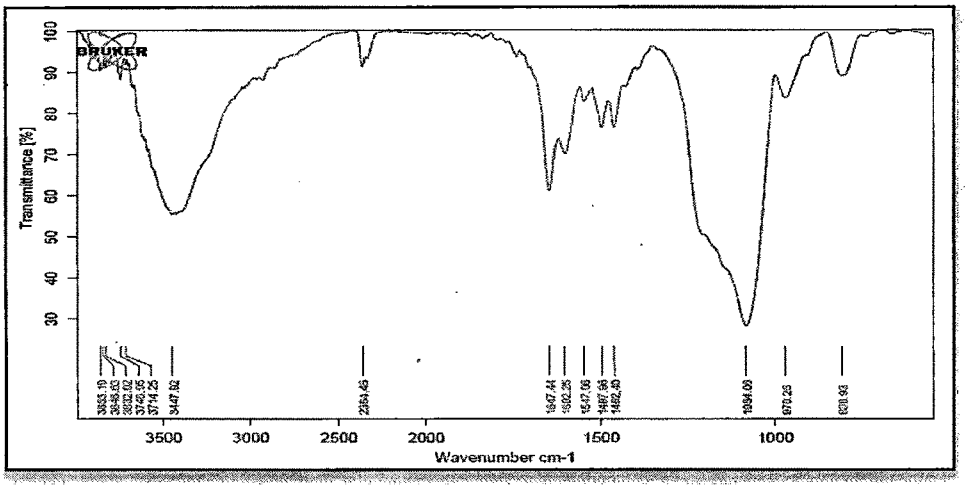

Figure 8.18: FTIR spectra of DTB loaded MSU-H MSNs

8.4.3.5 Differential scanning calorimetry (DSC)

DSC thermograms were obtained to study the effectiveness of drug loading. The absence of endothermic peak in drug loaded MSNs is the indicative of the amorphous state as drug is confined within the pores.

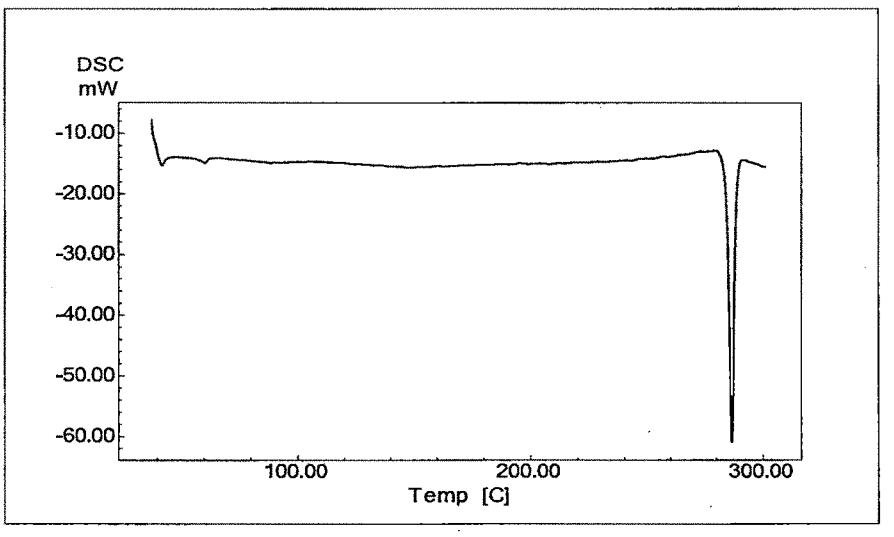

Figure 8.19: DSC thermogram of DTB

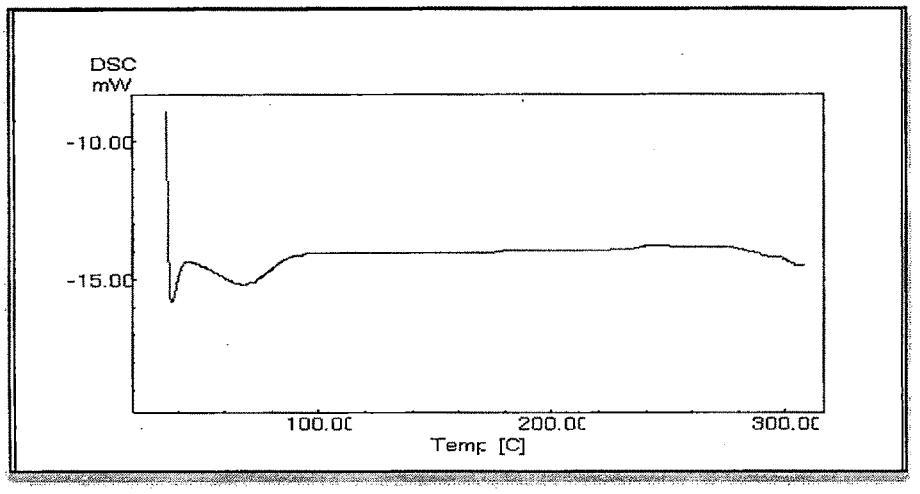

Figure 8.20: DSC thermogram of MSU-H MSNs

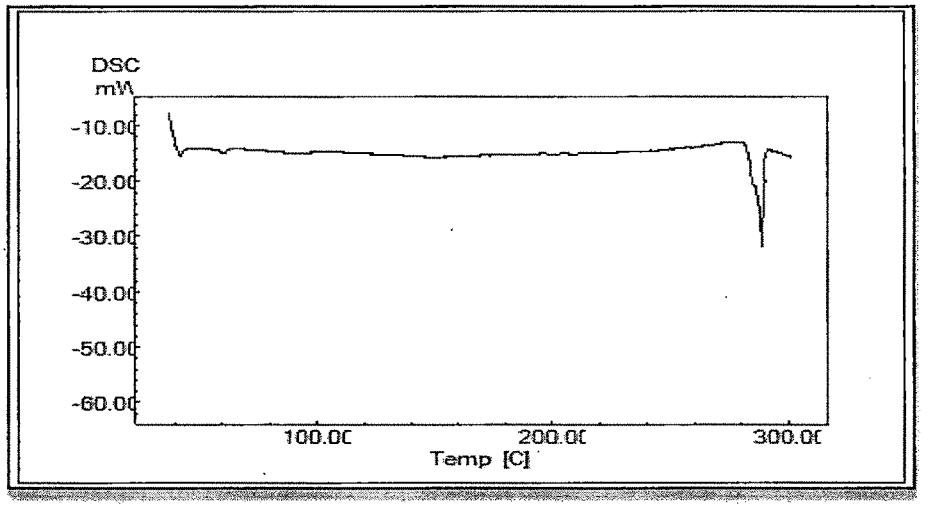

Figure 8.21: DSC thermogram of physical mixture of DTB and MSU-H MSNs

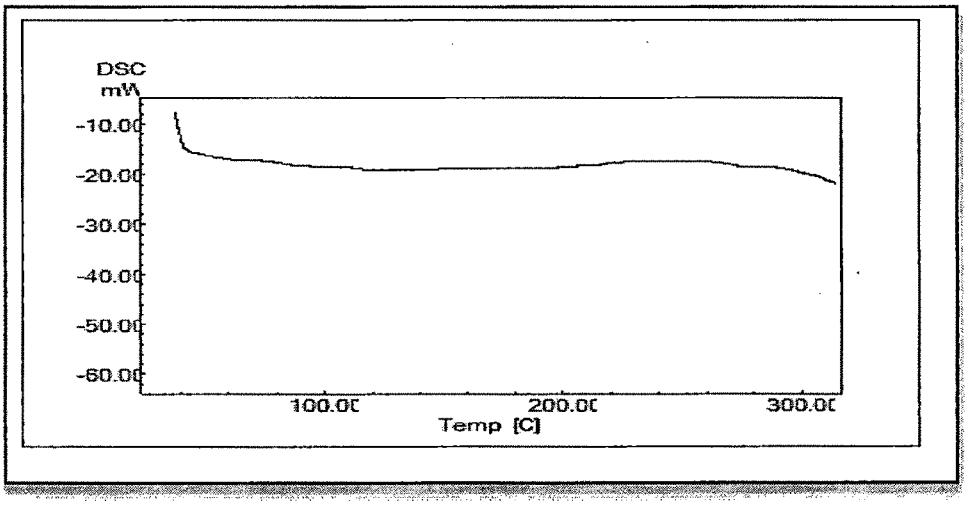

Figure 8.22: DSC thermogram of DTB loaded MSU-H MSNs

Figure 8.19-8.22 show DSC thermograms of MSU-H MSNs, drug (DTB) loaded MSU-H MSNs, physical mixture, and crystalline DTB. The DSC curve of DTB exhibited a single endothermic peak at 287 °C, which corresponded to its intrinsic melting point. Physical mixture of drug and MSNs show the less intense peak at 287 °C, indicating that drug molecules are not confined within the pores and drug was present in it crystalline state. However, no melting peak of DTB was identified in the DSC curves obtained from drug loaded MSNs. The absence of phase transitions owing to DTB in the DSC analysis is evidence that DTB is in a non-crystalline state.

8.5 *In-Vitro* dissolution study

Dissolution tests were performed at different pH conditions in order to investigate the drug release behavior in different regions of gastrointestinal tract. DTB dissolution from MSU-H-DTB was compared with those from DTB crystalline powder, physical mixture and marketed formulation (Fig. 8.24 (a–e)). In all test conditions DTB release from MSU-H MSNs had a more rapid burst effect[13-16] than the pure powder, physical mixture and marketed formulation. Schematic presentation of drug release from MSU-H MSNs was shown in Fig. 8.23.

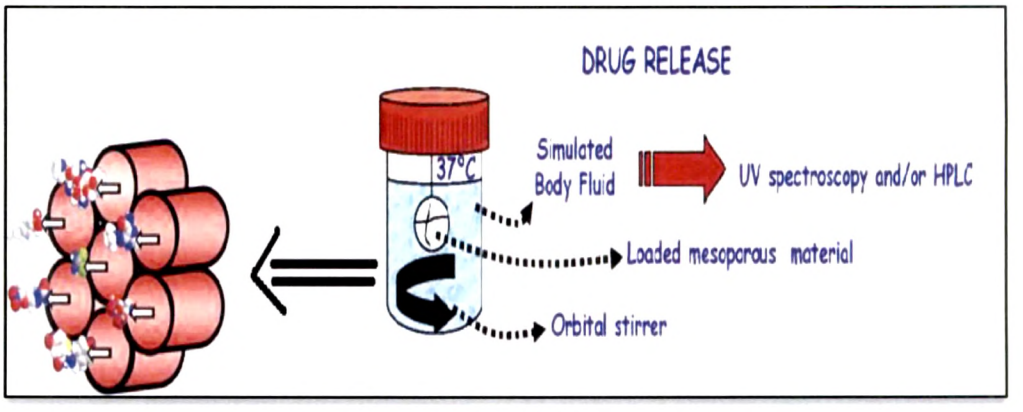

Figure 8.23: Schematic presentation of drug release from MSU-H MSNs

Table 8.9 and 8.10 show the DTB release percentages at the tested pHs after 10 and 30 min. respectively. The solubility of DTB is pH dependent; it can be observed that rapid release of the drug was more prominent in acidic media. In fact, in Acetate buffer pH 4 + Triton X-100 (1%) medium, more than 79% of drug was released from MSU-H-DTB and a complete drug (100%) release was obtained after 10 and 30 min, whereas DTB dissolution from the crystalline powder was as low as 8% and 42% after 10 and 30 min respectively.

Table 8.9: Percentage of drug release after 10 minutes

Dissolution media	% drug release			
	Crystalline drug	Physical mixture	Marketed formulation	Developed formulation
Simul. gastric fluid pH 1.2	48.468	54.611	56.166	87.003
Phosphate buffer pH 4.5	2.202	21.625	41.891	67.035
Phosphate buffer pH 6.8	3.650	6.859	17.549	50.622
Simul.intest. fluid pH 7.4	0.066	7.059	12.041	30.288
Acetate buffer pH 4 + Triton X-100 (1%)	8.338	31.623	51.962	79.819

Table 8.10: Percentage of drug release after 30 minutes

Dissolution media	% drug release			
	Crystalline drug	Physical mixture	Marketed formulation	Developed formulation
Simul. gastric fluid pH 1.2	50.224	63.708	78.934	100.000
Phosphate buffer pH 4.5	35.312	43.985	64.356	91.045
Phosphate buffer pH 6.8	12.803	20.497	39.109	90.300
Simul. Intest. fluid pH 7.4	2.209	10.990	16.032	90.182
Acetate buffer pH 4 + Triton X-100 (1%)	42.804	78.824	88.101	100.000

Finally, the DTB dissolution profile from MSU-H–DTB was compared to that of DTB from commercial formulation. The dissolution profiles indicate that after the 10 min drug release was more than 79% from MSU-H–DTB whereas only 51% in comparison with market formulation. Similarly after 30 min drug release from marketed formulation was found to be 88% whereas complete drug release was obtained from the developed formulation.

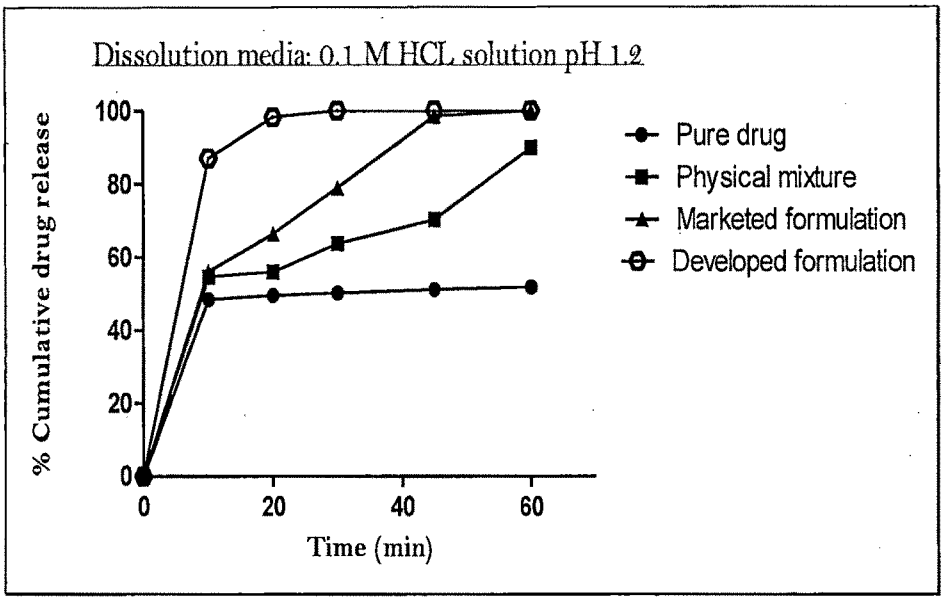

Figure 8.24-a: Release profile of DTB from crystalline DTB, physical mixture, marketed formulation, and developed formulation in pH 1.2

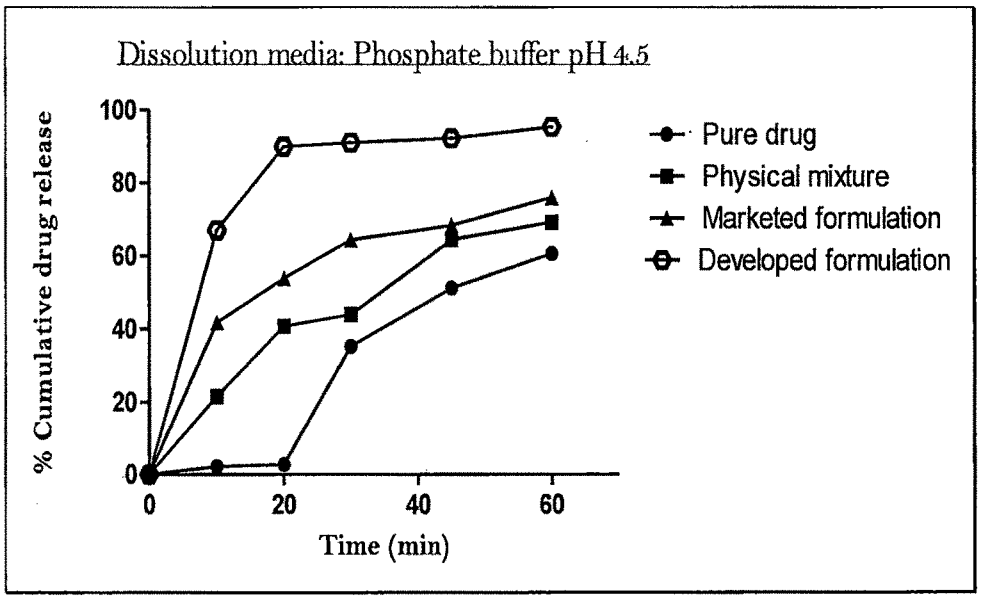

Figure 8.24-b: Release profile of DTB from crystalline DTB, physical mixture, marketed formulation, and developed formulation in pH 4.5

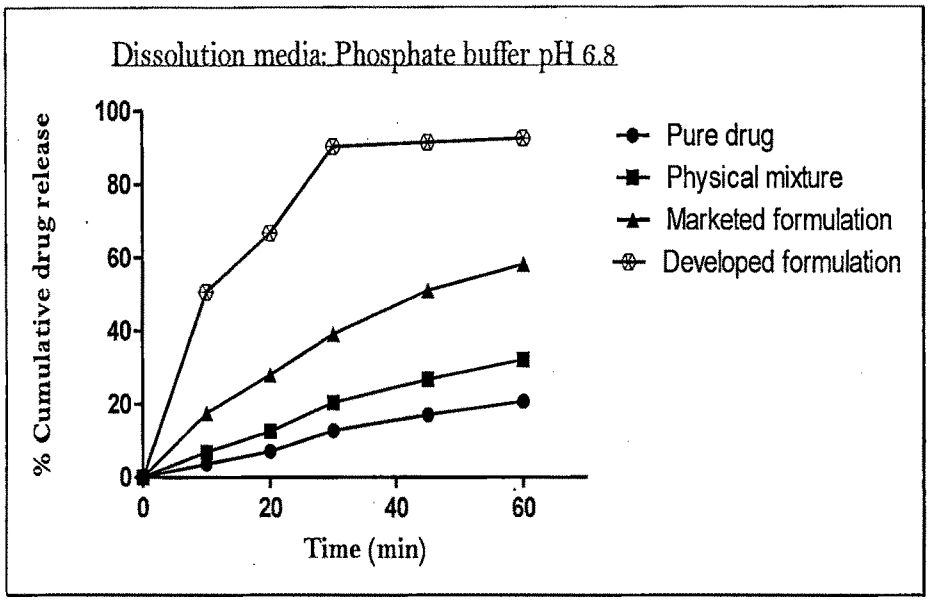

Figure 8.24-c: Release profile of DTB from crystalline DTB, physical mixture, marketed formulation, and developed formulation in pH 6.8

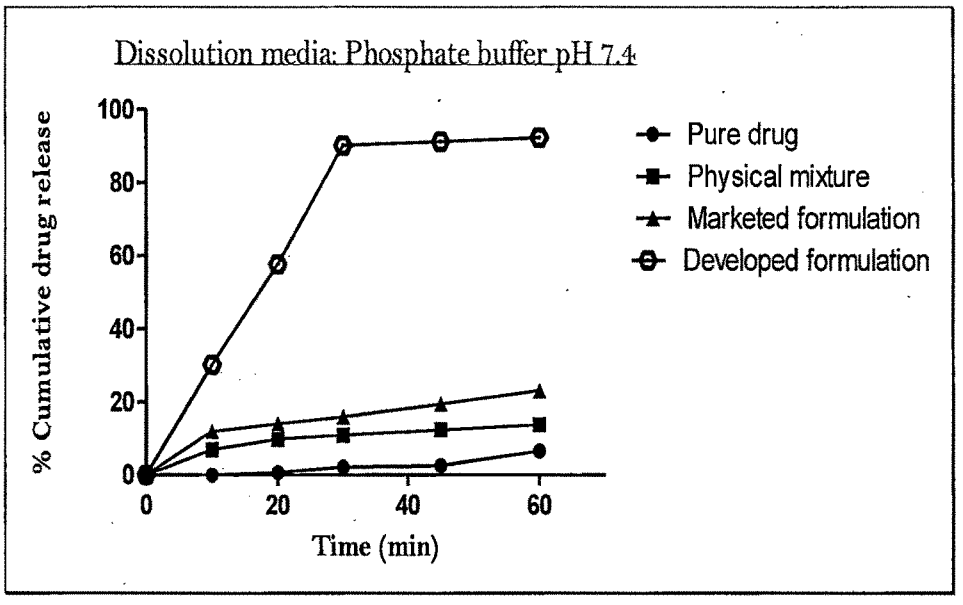

Figure 8.24-d: Release profile of DTB from crystalline DTB, physical mixture, marketed formulation, and developed formulation in pH 7.4

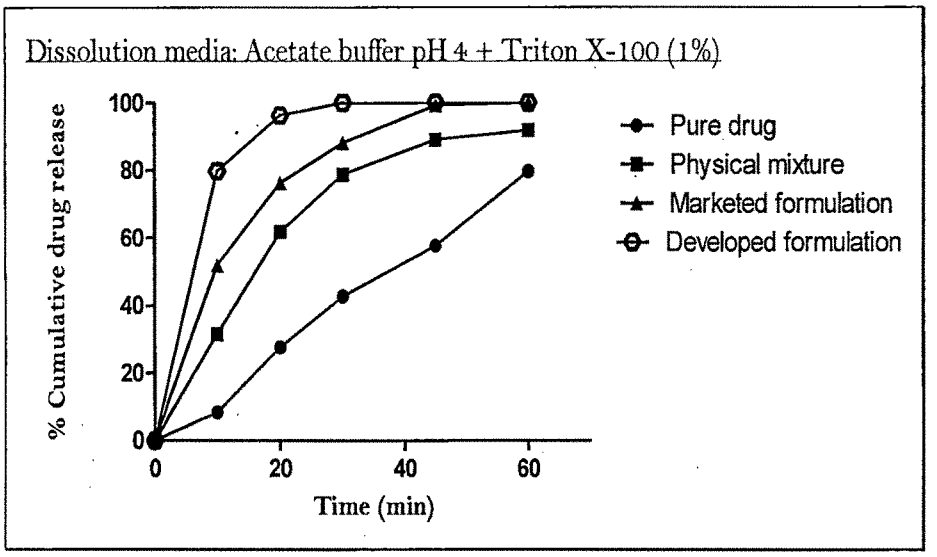

Figure 8.24-e: Release profile of DTB from crystalline DTB, physical mixture, marketed formulation, and developed formulation in reported media

References:

1 Wujun Xu, Qiang Gao, Yao Xua, Dong Wu, Yuhan Sun, Wanling Shen, Feng Deng. Controllable release of ibuprofen from size-adjustable and surface hydrophobic mesoporous silica spheres. Powd Tech. 2009; 191: 13-20.

2 Fish WP, Young J, Shah P, Gao Z. The use of experimental design principles in dissolution method development: development of a discriminating dissolution method for sprycel film-coated tablets. J Pharm Innov. 2009; 9: 9071-9075.

3 Ambrogia V, Perioli L, Marmottinib F, Giovagnolia S, Espositoa M, Rossia C. Improvement of dissolution rate of piroxicam byinclusion into MCM-41 mesoporous silicate. Eur J pharm Sci. 2007; 32: 216–222.

4 Haoualaa A, Zanolaria B, Rochatb B, Montemurrod M, Zamand K, Duchosale MA, Risc HB, Leyvrazd S, Widmera N, Decosterda LA. Therapeutic drug monitoring of the new targeted anticancer agents imatinib, nilotinib, dasatinib, sunitinib, sorafenib and lapatinib by LC tandem mass spectrometry. J Chromatogr B. 2009; 877: 1982–1996.

5 Griesser U.J, The importance of solvates. In Hilfiker R, ed. Polymorphism. Wiley-VCH Verlag GmbH & Co. KGaA, Weinheim, 2006; 211–233.

6 CRC handbook of solubility parameters and other cohesion parameters, A. F. M. Barton, ed., 2nd ed., CRC Press cop, Boca Raton (FL), 1991.

7 Bhattachar SN, Deschenes LA, Wesley JA. Solubility: it's not just for physical chemists. Drug Dis Today. 2006; 11: 1012–1018.

8 Bennema P, Van J, Van W, Los JH, Meekes H. Solubility of molecular crystals: Polymorphism in the light of solubility theory. Int J Pharm. 2008; 351: 1–2, 74–91.

9 Vandervoort J, Ludwig A. Preparation factors affecting the properties of polylactide nanoparticles: a factorial design study. Pharmazie. 2001; 56: 484- 488.

10 Box G, Hunter W, Hunter J. Statistics for experiments, John Wiley and Sons, New York, 1978; 291–334.

11 Cochran W.G, Cox G.M. Experimental Designs, second ed., John Wiley and Sons, New York, 1992; 335–375.

12 Brunauer S, Emmet P, Teller E. Adsorption of gases in multi molecular layers. J Am Chem Soc. 1938; 60: 309–319.

13 Salonen J, Laitinen L, Kaukonen AM, Tuura J, Björkqvist M, Heikkilä T, Vähä-Heikkilä K, Hirvonen J, Lehto V.P. Mesoporous silicon microparticles for oral drug delivery: loading and release of five model drugs. J Control Rel. 2005; 108: 362–374.

14 Heikkilä T, Salonen J, Tuura J, Kumar N, Salmi T, Murzin D.Y, Hamdy M.S, Mul G, Laitinen L, Kaukonen A.M, Hirvonen J, LehtoV. Evaluation of mesoporous TCPSi, MCM-41, SBA-15, and TUD-1 materials as API carriers for oral drug delivery. Drug Deliv. 2007; 14: 337–347.

15 Vasconcelos T, Sarmento B, Costa P. Solid dispersions as strategy to improve oral

bioavailability of poor water soluble drugs. Drug Discov Today. 2007; 12: 1068–1075.

16 Kesisoglou F, Panmai S, Wu Y. Nanosizing. Oral formulation development and biopharmaceutical evaluation. Adv Drug Deliv Rev. 2007; 59: 631–644.